EFFECT OF CONTACT ANGLE HYSTERESIS ON DROPLET BEHAVIORS: TWO-PHASE LATTICE BOLTZMANN SIMULATION

Wang Lei(汪磊)[1], *Xu Changyue*(许常悦)[1,2]

(1. Department of Modern Mechanics, University of Science and Technology of China, Hefei, 230026, P. R. China;
2. College of Aerospace Engineering, Nanjing University of Aeronautics and Astronautics, Nanjing, 210016, P. R. China)

Abstract: An approach of dealing with contact angle hysteresis in lattice Boltzmann method is introduced in detail. The approach is also used to investigate droplet behaviors on surfaces of chemical inhomogeneities or roughness (non-ideal surfaces). Droplet slipping on surfaces under gravity or in shear flows, and droplet impacting on surfaces are numerically simulated. It is found that the present approach is suitable to model droplet motions on non-ideal surfaces and the contact angle hysteresis has an obvious effect on the motion of droplets.

Key words: lattice Boltzmann; multiphase; contact angle hysteresis; droplet behaviors

CLC number: O359$^+$.1 **Document code**: A **Article ID**: 1005-1120(2013)03-0270-06

INTRODUCTION

Droplet slipping on a solid wall is a common phenomenon in nature and in engineering applications, such as water droplets hanging on glass, crude oil attached on rocks, pesticide spread over plants, and so on. These problems can be described as a droplet on a non-ideal wall with contact angle hysteresis, which is measured by two parameters: receding angle and advancing angle (denoted by θ_R, θ_A, respectively). In previous publications, there are lots of numerical and experimental studies on this topic. For instance, Kim, et al used the model of Inamuro, et al[1] to investigate water droplet properties on rough surfaces with periodical distributions of pillars[2]. Kusumaatmaja and Yeomans studied the droplet deformation when it passed through an array of hydrophilic stripes of different widths[3]. Varnik, et al investigated the droplet movement when it passed through stripes with different wetting properties[4]. However, most of the above studies intend to investigate contact angle hysteresis microscopically. All the same, it can be inferred that contact angle hysteresis may have an impact on the droplet dynamics. Different from the above investigations from microscopic view, here we focus on the macroscopic characteristic of hysteresis directly, regardless of the microscopic roughness. In order to investigate how the contact angle hysteresis affects the droplet dynamics, we numerically test droplet sticking or slipping on surfaces under gravity, two droplets coalescing on surfaces by surface tension and droplet impacting dynamics. In simulations, the lattice Boltzmann method that accounts for contact angle hysteresis is used[5]. The numerical method will be described in detail in the second part.

1 MATHEMATICAL FORMULATION AND NUMERICAL METHODS

1.1 Lattice Boltzmann method for two-phase flows

The multiphase Lattice Boltzmann method (LBM) used here was proposed by He, et al, in

Received date: 2013-04-08; **revision received date**: 2013-07-19

Corresponding author: Xu Changyue, Associate Professor, E-mail: cyxu@nuaa.edu.cn.

which an index function is used to track interfaces between liquid and gas[6]. Two distribution functions $\overline{f_i}$ and $\overline{g_i}$ are introduced to recover the Cahn-Hilliard equation (evolution of the index function) and Navier-Stokes equations, respectively

$$\overline{f_i}(\boldsymbol{x}+\boldsymbol{e}_i\delta t,\ t+\delta t)-\overline{f_i}(\boldsymbol{x},t)=-\frac{\overline{f_i}(\boldsymbol{x},t)-f_i^{\mathrm{eq}}(\boldsymbol{x},t)}{\tau}-\frac{(2\tau-1)}{2\tau}\frac{(\boldsymbol{e}_i-\boldsymbol{u})\cdot\nabla\psi(\phi)}{RT}\Gamma_i(\boldsymbol{u})\delta t \tag{1}$$

$$\overline{g_i}(\boldsymbol{x}+\boldsymbol{e}_i\delta t,t+\delta t)-\overline{g_i}(\boldsymbol{x},t)=-\frac{\overline{g_i}(\boldsymbol{x},t)-g_i^{\mathrm{eq}}(\boldsymbol{x},t)}{\tau}+\frac{(2\tau-1)}{2\tau}(\boldsymbol{e}_i-\boldsymbol{u})\cdot[\Gamma_i(\boldsymbol{u})(\boldsymbol{F}_s+\boldsymbol{G})-(\Gamma_i(\boldsymbol{u})-\Gamma_i(0))\psi(\rho)]\delta t \tag{2}$$

where τ is the relaxation time, which is related to kinematic viscosity ν by $\nu=c_s^2(\tau-0.5)\delta t$, $RT=\frac{1}{3}$, $\boldsymbol{x}$ the position of the node, t the time, δt the time interval, and $\boldsymbol{e}_i$ the discrete velocity. For D2Q9 model, $\boldsymbol{e}_i$ can be given as $[e_0,e_1,e_2,e_3,e_4,e_5,e_6,e_7,e_8]=\begin{bmatrix}0,1,0,-1,0,1,-1,-1,1\\0,0,1,0,-1,1,1,-1,-1\end{bmatrix}$. $\boldsymbol{F}_s=\kappa\rho\nabla\nabla^2\rho$, is the surface tension, κ the strength of the surface tension, ρ the density, $\boldsymbol{G}$ the body force. The above variables ν,τ,ρ can be derived by this unified form $\chi=\chi_L+\frac{\varphi-\varphi_{\min}}{\varphi_{\max}-\varphi_{\min}}(\chi_L-\chi_G)$, where "L" and "G" mean "liquid phase" and "gas phase", respectively. The equilibrium distribution functions f_i^{eq} and g_i^{eq} can be computed as

$$f_i^{\mathrm{eq}}(\boldsymbol{x},t)=\omega_i\phi\left[1+\frac{3\boldsymbol{e}_i\cdot\boldsymbol{u}}{c^2}+\frac{(3\boldsymbol{e}_i\cdot\boldsymbol{u})^2}{2c^4}-\frac{3\boldsymbol{u}^2}{2c^2}\right] \tag{3}$$

$$g_i^{\mathrm{eq}}(\boldsymbol{x},t)=\omega_i\left[p+\rho c_s^2\left(\frac{3\boldsymbol{e}_i\cdot\boldsymbol{u}}{c^2}+\frac{(3\boldsymbol{e}_i\cdot\boldsymbol{u})^2}{2c^4}-\frac{3\boldsymbol{u}^2}{2c^2}\right)\right] \tag{4}$$

where ϕ and p are the index function and the pressure, respectively, $\omega_0=\frac{4}{9},\omega_{1-4}=\frac{1}{9},\omega_{5-9}=\frac{1}{36}$, $c=\frac{\delta x}{\delta t}$, and δx is the lattice spacing. The macroscopic variables can be obtained by

$$\phi=\sum\overline{f_i} \tag{5}$$

$$p=\sum\overline{g_i}-\frac{1}{2}\boldsymbol{u}\cdot\nabla\psi(\rho)\delta t \tag{6}$$

$$\rho RT\boldsymbol{u}=\sum\boldsymbol{e}_i\overline{g_i}+\frac{RT}{2}(\boldsymbol{F}_s+\boldsymbol{G})\delta t \tag{7}$$

In the model, we set $\phi_{\max}=0.251$, $\phi_{\min}=0.024$, $\rho_L=0.251$, $\rho_G=0.024$[7].

1.2 Contact angle hysteresis

For a non-ideal solid wall, the contact angle hysteresis should be taken into consideration. Here, the geometric formulation is adopted to simulate the hysteresis effect. The formulation is given as[8]

$$\phi_{i,1}=\phi_{i,3}+\tan\left(\frac{\pi}{2}-\theta\right)\mid\phi_{i+1,2}-\phi_{i-1,2}\mid \tag{8}$$

where the first and the second subscripts of ϕ denote the coordinates along and normal to the solid boundary, respectively, θ is the apparent contact angle. In order to calculate the terms of $\nabla\psi(\phi)$ and $\nabla\psi(\rho)$, a layer of ghost cells adjacent to the solid boundary are necessary. The values of $\phi_{i,0}$, which is defined on the ghost cells, are given by $\phi_{i,0}=\phi_{i,1}$. To simulate the hysteresis effect, at each time step of computation, the local apparent contact angle at the contact points should be obtained first, then θ are compared with θ_R and θ_A. If $\theta\leqslant\theta_R$, θ in Eq. (8) should be replaced by θ_R; If $\theta\geqslant\theta_A$, θ in Eq. (8) should be replaced by θ_A; else, θ in Eq. (8) remains unchanged[9-10]. Here we can see that the hysteresis effect is prescribed by two parameters: Advancing angle and receding angle, which depend on the properties of fluids and solids.

2 RESULTS AND DISCUSSION

In this section, the ability of the scheme is used to model contact line dynamics on a non-ideal solid wall with contact angle hysteresis.

2.1 Droplet slipping on wall under gravity

Simulations of a droplet on the inner wall in a channel are conducted. The rectangular computational grids are $L\times H=251$ lattice unit$\times 71$ lattice unit, where lattice unit is abbreviated as l. u. and the initial radius of the semicircle droplet is 35 l. u.. The right and the left boundaries are solid walls and simple bounce-back is applied. Periodic boundary conditions are applied on the top and the bottom boundaries. The direction of the

gravity is vertical. There are four typical motion modes of the contact points due to four specified hysteresis windows. In Fig. 1(a), both the upstream and the downstream contact angles are always inside the hysteresis window (0°,180°), so the two corresponding contact points are always pinned on the wall. In Fig. 1(b), the upstream contact angle varies from the right angle to the acute angles, so it is always in the range of (0°, 110°). Consequently, the upstream contact line can not move. For the downstream contact point, at early stages it is pinned as the contact angle is less than 110°, and later it moves due to the contact angle greater than 110°. In Fig. 1(c), the downstream contact angle varies from the right angle to the obtuse angles which are always in the range of (70°,180°), so the downstream contact point remains immobile. For the upstream contact point, at early stages it is pinned due to the contact angle greater than 70°, and later it moves due to the contact angle less than 70°. Fig. 1(d) shows that at early stages the droplet deforms and keeps pinned. Subsequently the two contact angles do not fall into the specified hysteresis window and the whole droplet slips.

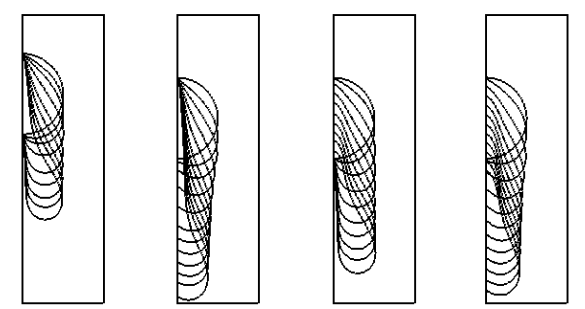

Fig. 1 Four typical motion modes of contact points under gravity with contact angle hysteresis considered

Through the above tests, it is found that the contact angle hysteresis effect has been qualitatively achieved. As we know, contact angle hysteresis is mainly caused by surface roughness or chemically inhomogeneity, which may prevent the motion of a droplet on these non-ideal surfaces. In order to validate this point, we investigate the behaviors of a 2-D droplet slipping on the inner wall in an inclined channel. The tilted angle is 55°, and the direction of gravity is vertical downward. The boundary conditions in the inlet and the outlet of the channel are periodic. Fig. 2 shows the typical droplet profiles at different time steps(t. s.) in slipping process. As shown in Fig. 2, initially, the droplet is located at the top part of the channel, then slips along the inwall under gravity, and finally reaches steady state. Because the whole droplet moves downward, the apparent contact angles at the downstream and the upstream contact points are 20° and 65°, respectively.

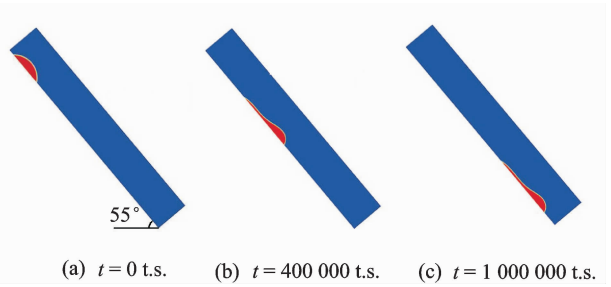

Fig. 2 Typical droplet profiles in slipping process($\theta_A=20°,\theta_A=65°$)

The distance between the two contact points is called wetting length(L) and the initial wetting length is L_0. The advancing angle is fixed at 65°. By varying the receding angles, we conducted seven computational cases to study the effect of hysteresis window on the relative wetting length L/L_0. Two important dimensionless parameters are defined as

$$Bo=\rho_L g L_0^2/\sigma, \quad Re=L_0\sqrt{gL_0}/\nu_L$$

where σ denotes the surface tension, ν_L the kinematic viscosity of droplet, and g the gravity. The dynamic viscosity ratio between the droplet and the ambient fluid is 10.46. In the simulations, $Bo=4.41$, $Re=29.35$. From Fig. 3, it is found that the relative wetting length diminishes with

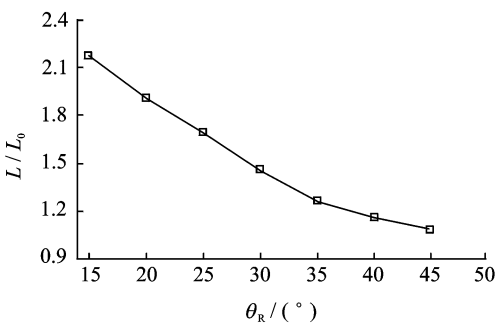

Fig. 3 Relative wetting length as function of receding angle($\theta_A=65°$, $Bo=4.41$, $Re=29.35$)

the increase of receding angle. In other words, the narrower the hysteresis window is, the shorter the relative wetting length is. The contact angle hysteresis window has a obvious effect on the relative wetting length. Indeed, we can easily find that the contact angle hysteresis has a tendency to prevent the droplet detaching from the wall.

2.2 Coalescence of two droplets on substrate

As we know, due to the action of surface tension, two initially hemisphere droplets on substrate would contact and coalesce. In this part, we investigate the effect of contact angle hysteresis on the coalescence dynamics of the above two droplets on the substrate. The rectangular computational grids are $Lx \times Ly \times Lz = 200$ l. u. $\times$ 75 l. u. $\times$ 60 l. u., and the initial radius of the hemisphere droplet is $R_0 = 30$ l. u. Two cases are conducted and compared. Figs. 4(a—b) are obtained through setting hysteresis window as $[30°, 40°]$ and $[30°, 70°]$, respectively. In simulations the nondimensional number Oh is defined as $Oh = \mu_L / \sqrt{R_0 \sigma \rho_L}$, and we set a $Oh = 0.1$, $\tau_L = \tau_G 0.6$. The 3-D subfigures in each column of Fig. 4 shows the droplets coalescing processes driven by surface tension and the snapshots are chosen at the same moment for comparison. The subfigures on the bottom of each column are the corresponding traces of the droplet contact lines. It is found that from $t = 0$ t. s. to $t = 2\,000$ t. s. the whole contact lines expand with contact angle equal to

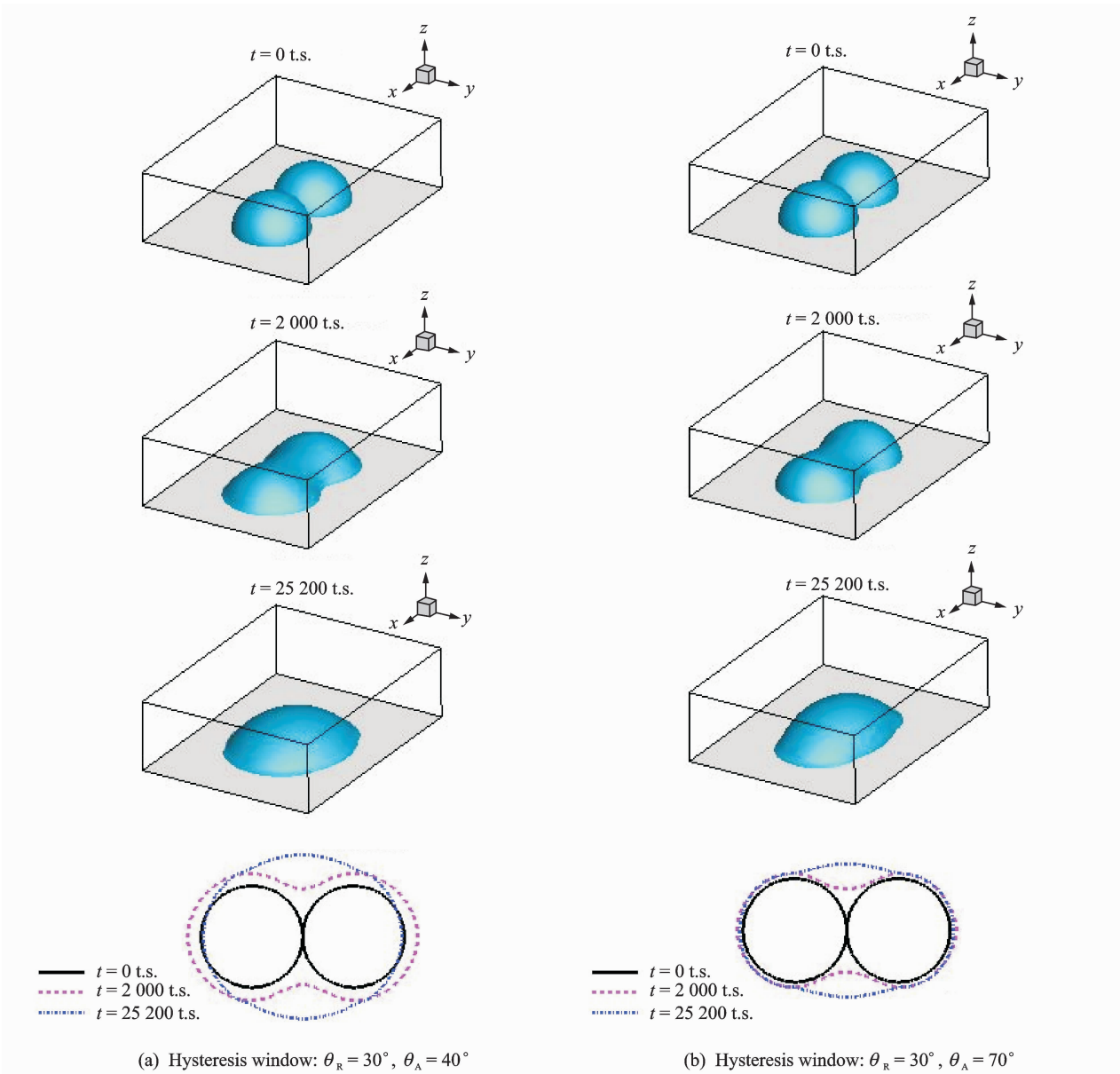

(a) Hysteresis window: $\theta_R = 30°$, $\theta_A = 40°$ (b) Hysteresis window: $\theta_R = 30°$, $\theta_A = 70°$

Fig. 4 Comparisons of coalescence process of two 3-D hemispherical droplets driven by surface tension

θ_A, but from $t=2\ 000$ t. s. to $t=25\ 200$ t. s. the contact lines around the right and the left end begin to recede with contact angle equal to θ_R and the intermediate contact lines continue expanding with contact angle equal to θ_A. Therefore, when the final merged droplet has reached equilibrium state, its shape does not retain sphere due to contact angle hysteresis effect. We can conclude that contact angle hysteresis obviously influences the dynamics of droplets coalescence.

2.3 Droplet impacting on solid wall

In this part, we mainly study the effect of contact angle hysteresis on the dynamics of a droplet impacting on a solid wall.

Two cases with different hysteresis windows are conducted, as shown in Fig. 5(a) $\theta_R=90°$, $\theta_A=90°$ and Fig. 5(b) $\theta_R=90°$, $\theta_A=130°$. Gravity is applied on the whole filed. The computational domain is 201 l. u. $\times$151 l. u., and the initial radius of the semicircle droplet is 30 l. u.. The distance between the initial droplet center and the wall is 100 l. u.. In each simulation, a droplet is released from the initial position. Then the droplet falls and moves towards the bottom wall under gravity. When it contacts with the wall, the droplet deforms and later relaxes towards equilibrium. Fig. 5 shows the droplet evolution process during the impaction. The pictures at $t=40\ 000$ t. s. are final steady states. It is found that the impacting dynamics is obviously influenced by contact angle hysteresis. The snapshots of the droplet profile at different time are shown in Fig. 5.

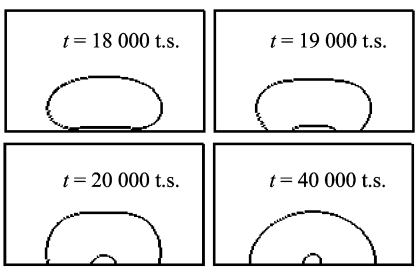

(a) $\theta_R=90°$, $\theta_A=90°$

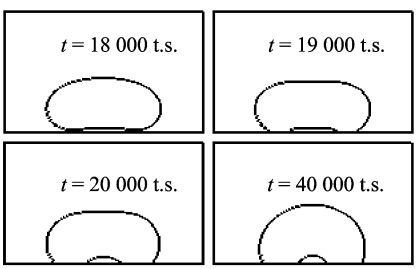

(b) $\theta_R=90°$, $\theta_A=130°$

Fig. 5 Comparisons of droplet impacting on wall between two hysteresis windows

For further quantitative comparison, a axisymmetric droplet normally impacting on a plane is simulated and well compared with the results from the experiment in Ref. [11]. Initially, the droplet contacts with the plane tangentially and has a normal velocity U. Two dimensionless parameters are

$$We=\rho_L U^2 R/\sigma, \quad Re=\rho_L UR/\mu_L$$

where R is the droplet radius, σ the surface tension and μ_L the dynamic viscosity of droplet. Fig. 6 shows the snapshots of droplet at different moments. r denotes the radial coordinate, and z the axial coordinate. The corresponding dimensionless time is $t'=t/t^*$. The red lines represent the droplet profiles obtained from simulations, and the black are images taken in the experiments in Ref. [10]. In both the simulations and the experiments, the viscosity ratio is $\mu_L/\mu_G=20$. Due to the limitation of numerical stability, the density ratio in the simulations is $\rho_L/\rho_G=10.46$, which is different from the density ratio $\rho_L/\rho_G=1\ 000$ in the experiments. This difference may lead to the fact that the droplet profiles obtained by simulations do not match the results from experiment

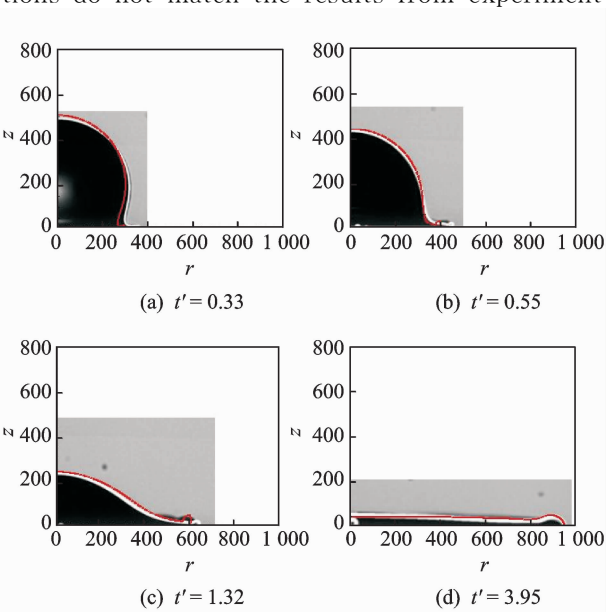

(a) $t'=0.33$ (b) $t'=0.55$

(c) $t'=1.32$ (d) $t'=3.95$

Fig. 6 Snapshots of droplet at different moments ($We=164$, $Re=457$, $\theta_R=13°$, $\theta_A=46°$)

accurately. However, it is believed that the discrepancy between simulations and experiments can be greatly reduced or ignored if the density ratio is higher.

3 CONCLUSION

The two-phase lattice Boltzmann method, i.e. the He-Chen-Zhang model, is applied to study droplet behaviours on non-ideal surfaces. For non-ideal surfaces, contact angle hysteresis is described by θ_R and θ_A. When a droplet is on the inner wall of a channel under gravity, four typical motion modes of contact points are observed. Furthermore, when a droplet is put on an inclind wall under gravity, it is found that the steady wetting length diminishes with the increment of contact angle hysteresis window. Coalescence of two droplets on substrate is also simulated and it is observed that the merged droplet appears different equilibrium state due to contact angle hysteresis. At last, a droplet impacting on a solid wall from some height is investigated. One can easily found that the contact angle hysteresis has an obvious effect on the impacting dynamics. Then the simulation results of droplet inertial-impacting on substrate are compared with that obtained from experiments, and very good agreement is found. Through the above tests, it is concluded that the present method can capture the behaviors of droplets on non-ideal walls, and indeed the contact angle hysteresis has an important impact on the dynamics.

References:

[1] Inamuro T, Ogata T, Tajima S, et al. A lattice Boltzmann method for incompressible two-phase flows with large density differences[J]. J Comput Phys, 2004, 198(2):628-644.

[2] Kim Y H, Choi W, Lee J S. Water droplet properties on periodically structured superhydrophobic surfaces a lattice Boltzmann approach to multiphase flows with high water air density ratio[J]. Microfluid Nanofluid, 2011, 10(1):173-185.

[3] Kusumaatmaja H, Yeomans J M. Controlling drop size and polydispersity using chemically patterned surfaces[J]. Langmuir, 2008, 23(2):956-959.

[4] Varnik F, Truman P, Wu B, et al. Wetting gradient induced separation of emulsions: A combined experimental and lattice Boltzmann computer simulation study[J]. Phys Fluids, 2008, 20(7): 072104-1-072117-14.

[5] Wang L, Huang H, Lu X. Scheme for contact angle and its hysteresis in a multiphase lattice Boltzmann method[J]. Phys Rev E, 2013, 87(1): 013301-1-013301-9.

[6] He X, Chen S, Zhang R. A Lattice Boltzmann scheme for incompressible multiphase flow and its application in simulation of rayleigh taylor instability [J]. J Comput Phys, 1999, 152(2): 642-663.

[7] Zhang R, He X, Chen S. Interface and surface tension in incompressible lattice Boltzmann multiphase model[J]. Comput Phys, Commun, 2000,129(1-3): 121-130.

[8] Ding H, Spelt P D M. Wetting condition in diffuse interface simulations of contact line motion[J]. Phys Rev E, 2007, 75(4): 046708-1-046708-8.

[9] Dupont J B, Legendre D. Numerical simulation of static and sliding drop with contact angle hysteresis [J]. J Comput Phys, 2010, 229(7):2453-2478.

[10] Spelt P D M. Level-set approach for simulations of flows with multiple moving contact lines with hysteresis[J]. J Comput Phys, 2005, 207(2): 389-404.

[11] Ding H, Theofanous T G. The inertial regime of drop impact on an anisotropic porous substrate[J]. J Fluid Mech, 2012, 691:546-567.

(Executive editor: Zhang Bei)